Response to Reviewer #1

Dear Reviewer:

We would like to thank you for the constructive comments and suggestions, which help to improve the quality of our work. We have replied each comment point-by-point and modified the manuscript. According to the suggestions, we have restated the scale-selective scheme and added more validation for the SEIA output. Now the time span of the dataset has been extended to 1993-2019. In addition, the systematic comparison between SEIA and existing eddy dataset has been added as well.

In the following responses, *the original comments are quoted in Italic font*, and the replies are in blue letters. Please check out the detailed responses to the comments below.

The suggestions are as follows:

(1) *The manuscript is lack of innovations and highlights. It attempts to make improvements for eddy identifying and tracking, including the scale-selective scheme in eddy detection and the overlap scheme in eddy tracking. But there are still some major parts need to be improved in the paper.*

We thank the reviewer for the constructive comments and suggestions, which have been considered carefully and responded to in detail.

(2) *The scale-selective scheme corresponds to the radius of eddies ranging from 25 to 125 km in the paper, which is incomprehensible. The formula as Line 161 shows present the scale-selective scheme, which means that you still select eddy contour by the threshold (Pmin-Pmax). However, the scale of eddy is changed with latitude, which should be considered in this paper.*

We feel sorry to make you confused. Actually, Chelton et al. (2011) suggest that global eddies have scales between 50 and 250 km (Fig. A1), which equals to 25 to 125 km for the radius of eddies ranging. The Pmin-Pmax principle of the scale-selective scheme is conducted for all the eddies in the global oceans but not eddies in certain

latitude or region. Chelton et al. (2011) further demonstrate that eddies with radius of 25 to 75 km account for 90% of global eddies. With one-core principle, for one SLA peak, there will be several contours centered it. The scale-selective scheme will choose the biggest contour as the 'edge' of the eddy, among which the Pmin-Pmax principle will make sure that such edge doesn't overestimate or underestimate the eddy impact area. Meanwhile, the Pmin is corrected considering the concept of eddy-like structure due to the input data resolution. That is, the scale-selective scheme (basically, the Pmin-Pmax principle) is utilized to ensure that the definition of eddy boundary varies with the development of eddy and does not fall into the extreme.

Indeed, the scale of eddy is changed with latitude. Taking the eddies in the north hemisphere in 2015 as example, the relationship between eddy radius and latitude is shown in Fig. A2. The geographical distribution of the mean eddy is characterized as an essentially monotonic decrease from about 0.65° in the near-equatorial regions to about 0.5° at 60° latitude in both hemispheres, which combine well with the results in Chelton et al. (2011). This in turn proves the validity of the scale-selective scheme, which does not remove the characteristic variation of the eddy radius with latitude.

However, after taking your comments into consideration, we have rewritten and reorganized the relevant content of the manuscript to better illustrate the scale-selective scheme.

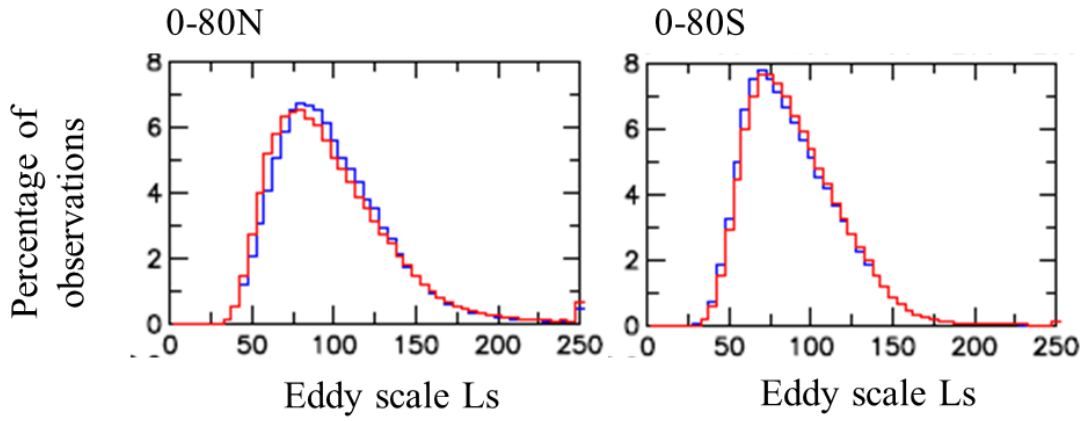

Figure A1. The distributions of the radius scales Ls of eddies with lifetimes ≥16 weeks in the northern (left) and the southern (right) hemispheres (Chelton et al., 2011).

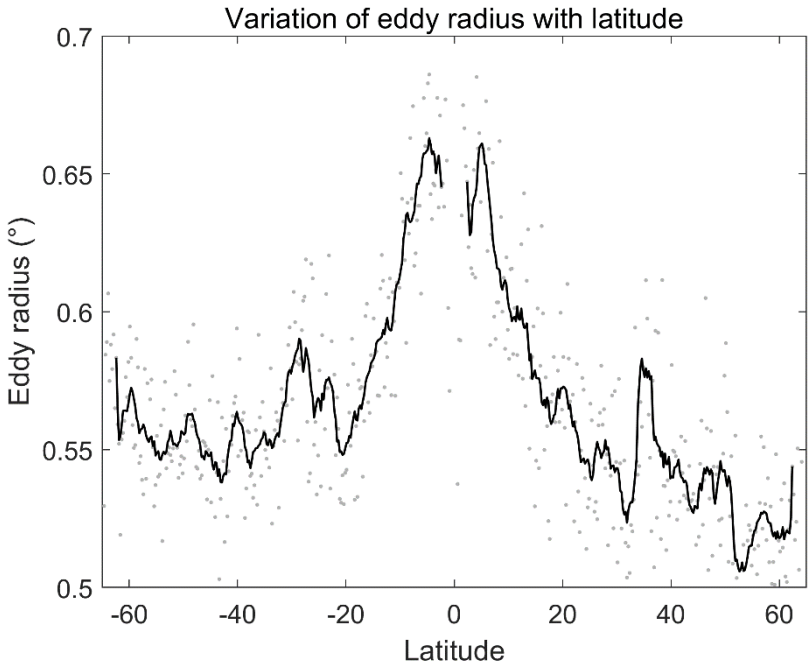

Figure A2. The relationship between eddy radius and latitude from the SEIA output in the north hemisphere in 2015.

Chelton, D. B., Schlax, M. G., and Samelson, R. M.: Global observations of nonlinear mesoscale eddies, Progress in Oceanography, 91, 167-216, 10.1016/j.pocean.2011.01.002, 2011.

(3) *The validation part is not sufficient. Other source of data should be considered in the validation, like remote sensing data (sst, sss or oceanic chlorophyll) and in situ data (drifter or argo).*

We feel sorry for the insufficient discussion of the SEIA eddy dataset. At your suggestion, we have added validation of the observations for the SEIA eddy dataset, including SMAP SSS and Argo data. Based on the 5-year output of the SEIA in the eastern tropical North Pacific Ocean (150°E-110°W, 10°-20°N) as an example, the SLA and geostrophic flow anomaly eddy composites are shown in Figure 8. The composite shows very clear signals: SLA and rotating fluid are nearly homogeneously distributed with the eddy centre (Figs. 8a and b). The in-phase variation between SLAs and geostrophic flow anomalies is a vivid manifestation of the geostrophic equilibrium

relationship.

Furthermore, the eddy-induced salinity variability in the eastern tropical North Pacific is characterized by a monopole mode for cyclonic eddies and a dipole mode for anticyclonic eddies (Figs. 8c and d), which differs from the results of Delcroix et al. (2019) that all eddies are monopole modes. The reason for this discrepancy may be that Delcroix et al. (2019) used high-pass filtered SLA data for eddy detection in their study.

Using Argo buoy data, we deeply explore the 3D structural features of eddies based on the SEIA output for the North Pacific region in 2015. The average temperature and salinity at 100 m inside both the anticyclonic and cyclonic eddy verify the classical theory of the eddy, i.e., the hydrological conditions inside the anticyclonic eddy tend to be warm and light, while those of the cyclonic eddy tend to be cold and salty (Fig. 9). On the other hand, the temperature and salt profiles inside the eddies indicate that the classic temperature and salt characteristics below the upper layer (100 m) no longer apply for both types of eddies, and the water masses inside the cyclonic eddies appear warmer and saltier (Fig. S2).

The above discussion demonstrates the accuracy of SEIA for eddy identification and proper tracking. The corresponding content now has been added in the revised manuscript.

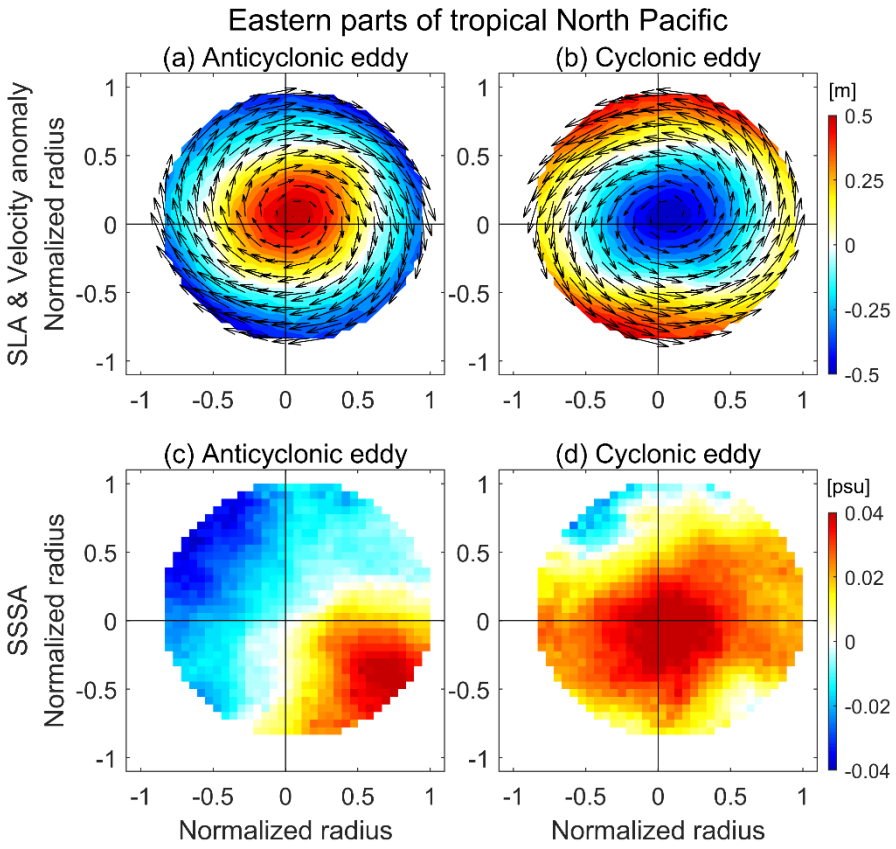

Figure 8. Distribution characteristics of the SLAs (shading, unit: m) and geostrophic velocity anomalies (arrow, unit: m/s) of (a) anticyclonic and (b) cyclonic eddy composites in the eastern parts of the tropical North Pacific. (c, d) Same, but for the sea surface salinity anomaly (SSSA).

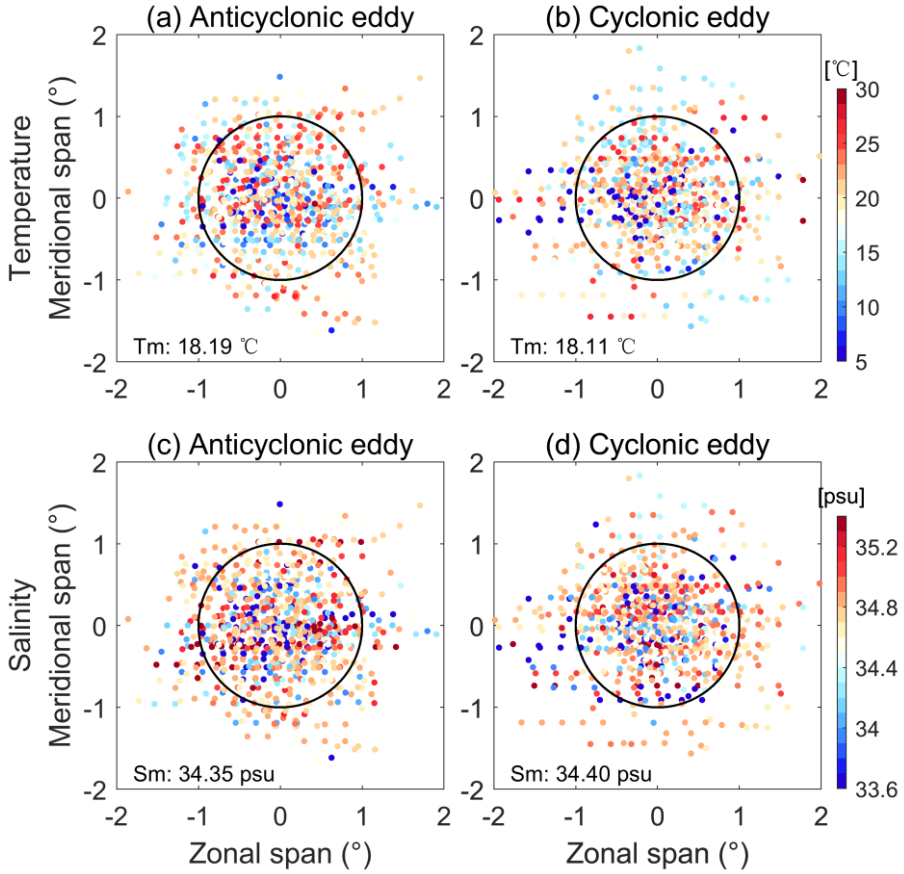

Figure 9. Scatter plots of the thermohaline inside eddies (at a depth of 100 m) based on Argo buoy data from the North Pacific in 2015: (a) anticyclonic eddy: temperature, (b) cyclonic eddy: temperature, (c) anticyclonic eddy: salinity, and (d) cyclonic eddy: salinity. The black circles denote a radius of 1° around the centre of each eddy composite. Tm and Sm are the average temperature (unit: °C) and salinity (unit: psu) inside the black circle, respectively.

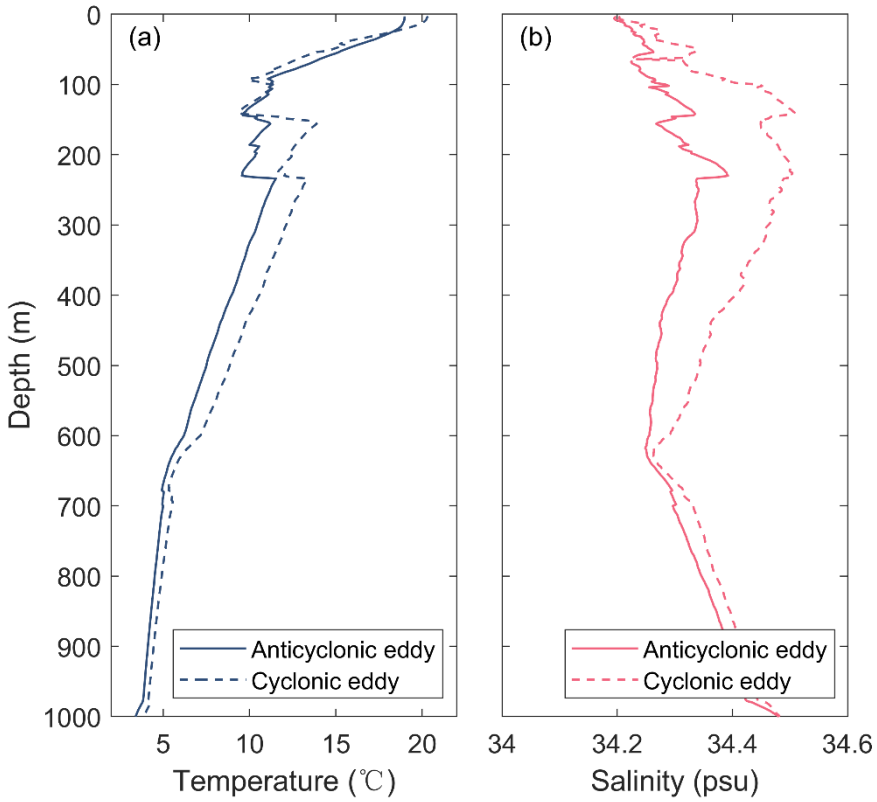

Figure S2. Temperature and salt profiles inside eddies based on Argo buoy data from the North Pacific in 2015: (a) temperature (unit: °C): the blue solid line and blue dashed line correspond to anticyclonic eddies and cyclonic eddies, respectively, (b) salinity (unit: psu): the red solid line and red dashed line correspond to anticyclonic eddies and cyclonic eddies, respectively.

(4) *In this paper, the data set of eddy during 2015-2019 are detected and tracked. The SLA data set from 1993 is available, which should be adopted to analysis. Meanwhile, the systematic comparison between eddy dataset in this paper and existing eddy datasets (like [1,2]) should be conducted in this work.*

Thanks for pointing this out. Now we have extended the time span of eddy identification to 1993-2019 and updated the repository (https://doi.org/10.11922/sciencedb.o00035.00004). The systematic comparison with the existing eddy datasets also has been conducted in the *application and validation* section. Figure 7 shows the eddy identification results in the SCS region on August 6, 1993, where the red and blue lines (dots) represent an anticyclone and a cyclone,

respectively.

As shown in the figure, the eddies are distributed throughout the SCS basin in a northeast–southwest trend, and they are mostly anticyclonic eddies. The W-A method is less capable of defining the eddy boundaries and tends to overestimate the eddy boundaries/radii, such as for the two anticyclonic eddies with abnormal bulges in the northern SCS (Figure 7a). In addition, the W-A method treats two weaker anticyclonic eddies in southwestern Taiwan as the same eddy. The Faghmous algorithm is more effective but still tends to overestimate the eddy impact area and identify relatively weak eddies (Fig. 7b). In contrast, the SEIA not only identifies a reasonable number of eddies but also defines boundaries more accurately without overestimation.

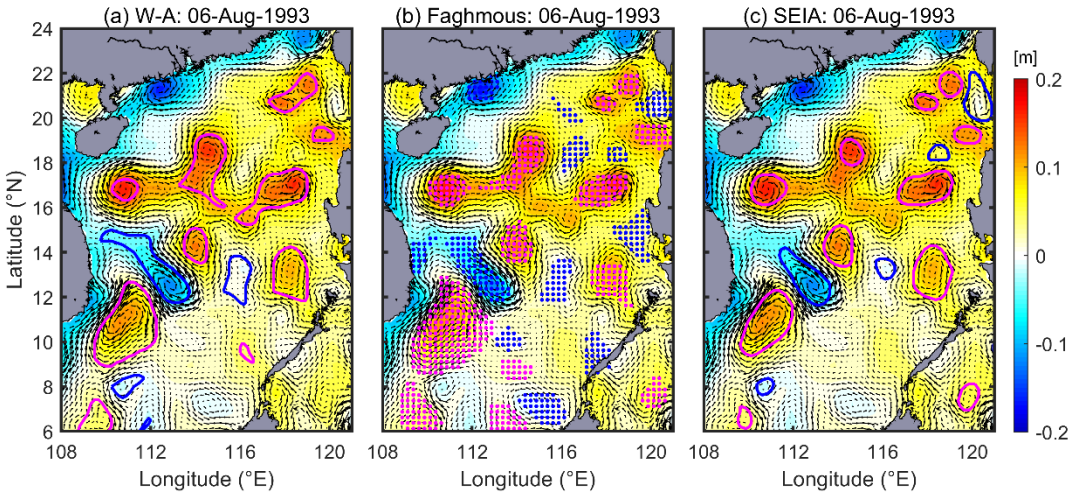

Figure 7. Detection results of the (a) W-A (Chen et al., 2011), (b) Faghmous (Faghmous et al., 2017) and (c) SEIA methods on August 6, 1993 in the South China Sea. The shading colors and arrows represent the SLA (unit: m) and geostrophic velocity anomaly, respectively. Red lines/dots represent the boundary/area of anticyclonic eddies, and the blue lines/dots for cyclonic eddies.

(5) *The manuscript is written very carelessly with many errors and unclear places. The level of English (grammar, style and syntax) throughout the manuscript does not meet the journal's required standard. I suggest rejecting the manuscript.*

We feel sorry for the English level problem of the manuscript. As non-native

English writers, we sent the manuscript to a specialized agency for grammatical corrections before submission, but we still apologize for the current situation. At your suggestion, we have rewritten some of the sentences that were not clearly described and corrected several errors. The revised manuscript was also sent for grammatical revision and we hope that it will now meet the journal's standards.